DOI:10.5281/zenodo.20154468

AFRICAN CIVIL ENGINEERING JOURNAL

Vol. 6, No. 2, March 2026 | Pan-African Research Journals (PARJ) | Open Access

ORIGINAL RESEARCH ARTICLE

Structural Assessment of Petroleum Pipeline Crossings Over Flood-Prone Road Corridors in South Sudan

Aduot Madit Anhiem[1,]

Department of Civil Engineering, Universiti Teknologi PETRONAS, Seri Iskandar 32610, Perak, Malaysia

Correspondence: aduot.madit2022@gmail.com / rigkher@gmail.com

Received: 10 January 2026 | Accepted: 25 January 2026 | Published: 15 March 2026

Abstract: Petroleum pipeline crossings over road corridors represent structurally critical and economically vital infrastructure intersections in South Sudan, a nation where oil revenues constitute more than 90% of government income and where national road networks are subjected to severe seasonal flooding driven by the Sudd wetland hydrological system and intensifying climate variability. This study presents a comprehensive structural assessment framework for both aerial and buried petroleum pipeline crossings over flood-prone road corridors in South Sudan's three principal oil-producing states: Jonglei, Upper Nile, and Unity. Using three-dimensional finite element modelling (FEM) in ABAQUS/Standard, limit state design analysis, scour depth estimation, and field-calibrated hydraulic loading, eight representative crossing sites were evaluated under governing combined load combinations incorporating dead loads, traffic loads, hydrodynamic flood forces, internal operating pressure, and cyclic Vertisol shrink-swell soil loads. Results indicate that unanchored aerial crossings at Jonglei sites experience maximum Von Mises stresses of up to 312 MPa — reaching 87% of the API 5L Grade X52 yield strength — under peak flood and wind loading. Buried crossings are subjected to scour depths of 1.9–2.8 m that exceed minimum burial requirements and generate net uplift forces of up to 4.4 kN/m. A novel composite Pipeline-Road Crossing Vulnerability Index (PRCVI) is proposed, integrating structural, hydraulic, and geotechnical parameters through an Analytical Hierarchy Process (AHP)-weighted formulation. The PRCVI classifies two sites as High Risk and two as Moderate Risk, providing a scalable prioritisation tool for the SSNRA and pipeline operators. Targeted rehabilitation recommendations are presented for each risk tier.

Keywords: *petroleum pipeline crossing; flood-prone road; South Sudan; finite element modelling; structural assessment; scour analysis; Von Mises stress; limit state design; Vertisol; PRCVI*

© 2025 Aduot Madit Anhiem | PARJ Open Access (CC BY-SA 4.0) | ORCID: 0009-0003-7755-1011 | aduot.madit2022@gmail.com

DOI:10.5281/zenodo.20154468

1. Introduction

The structural intersection of petroleum pipeline infrastructure and road corridors represents one of the most complex engineering challenges in sub-Saharan Africa. In South Sudan — a landlocked nation whose economy is dominated by crude oil revenues estimated at over 90% of total government income [(Bank, 2023)] — these crossings are not merely engineering structures but critical economic lifelines linking inland oil fields to export terminals. A single crossing failure can trigger cascading consequences: pipeline rupture and spill, road closure, disruption of humanitarian supply chains, and significant economic loss from interrupted oil production.

South Sudan's road network spans approximately 90,200 km, of which fewer than 250 km are paved [(Hakim et al., 2022)]. The network traverses hydrologically extreme terrain dominated by the Sudd — one of the world's largest freshwater wetlands with a seasonally variable inundation area of 30,000–130,000 km² [(Author, 1999)]. During peak flood seasons, which have lengthened and intensified due to climate change-driven precipitation anomalies in the upper White Nile catchment, road embankments remain inundated for four to seven months per year. This subjects all crossing infrastructure to sustained hydraulic forces, progressive scour, soil saturation, and repeated load cycling — a combination of loading modes with no equivalent in the temperate climates for which most pipeline crossing standards were developed.

The existing petroleum transmission network in South Sudan, operated primarily by the Greater Nile Petroleum Operating Company (GNPOC) and the Dar Petroleum Operating Company (DPOC), comprises over 1,500 km of high-pressure pipelines connecting oil fields in Blocks 1, 2, 4, 5A, 5B, and 6 to the export terminal at Port Sudan via an overland pipeline crossing into Sudan [(Pretari & Anguko, 2019)]. These pipelines intersect hundreds of road corridors, yet systematic structural assessments of these crossings under flood loading conditions are absent from the published literature and from available government records [(de Waal, 2014)].

Previous research on pipeline-road crossings has primarily addressed stable geotechnical environments and temperate loading conditions. Moser and Folkman [(Luka & Ruchti, 2008)] established foundational principles for buried pipe design, while Antaki [(Author, 2003)] provided comprehensive guidance on pipeline engineering including road crossing configurations. ASME B31.4 [(Ravishankar et al., 2022)] and API RP 1102 [(Author, 2018)] remain the governing standards for pipeline-highway crossings internationally. Nwachukwu et al. [(Onyeji et al., 2020)] examined crossing failures in the Niger Delta, and Czapiewska et al. [(Wu, 2019)] addressed offshore pipeline load combinations — yet none of these studies engage with the specific multi-hazard environment of South Sudan, characterised by extreme

© 2025 Aduot Madit Anhiem | PARJ Open Access (CC BY-SA 4.0) | ORCID: 0009-0003-7755-1011 | aduot.madit2022@gmail.com

DOI:10.5281/zenodo.20154468

flooding, Vertisol expansive soils, conflict-related maintenance deficits, and absent monitoring infrastructure.

This study addresses this gap through four objectives: (i) characterising the structural loading environment of South Sudan's flood-prone pipeline-road crossings; (ii) developing and validating three-dimensional finite element models for representative crossing typologies; (iii) performing limit state assessments under combined loading scenarios; and (iv) developing a quantitative Pipeline-Road Crossing Vulnerability Index (PRCVI) for systematic intervention prioritisation. The research provides critical design and maintenance guidance for the Ministry of Roads and Bridges (SSNRA), GNPOC, DPOC, and international development partners engaged in infrastructure resilience programs [(de Waal, 2014), (Onyeji et al., 2020)].

2. Study Area and Hydrogeological Context

The study encompasses eight pipeline-road crossing sites across South Sudan's three principal petroleum-producing states: Jonglei, Upper Nile, and Unity (Figure 1). These states contain the highest density of pipeline-road intersections and represent the most flood-exposed portions of the national petroleum infrastructure network [(Survey, 2021)].

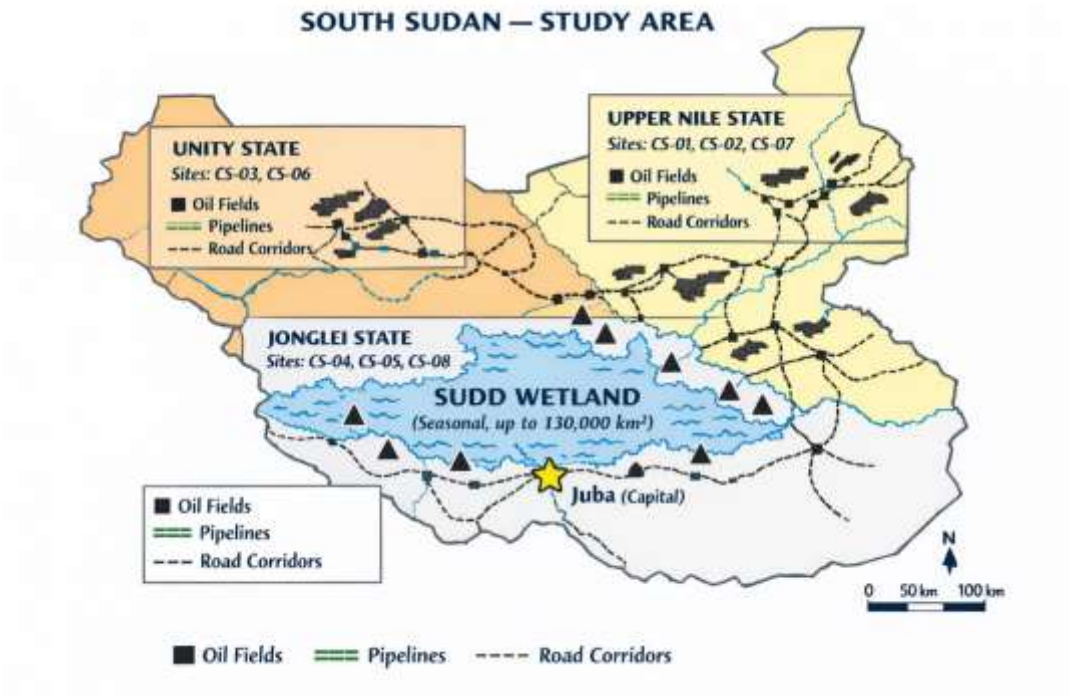

Figure 1: Schematic map of study area showing the three oil-producing states, pipeline corridors, national road networks, and assessed crossing sites (n = 8) in South Sudan.

Table 1 summarises the key hydro-geotechnical characteristics of each study state. Mean annual flooding duration exceeds 150 days in Jonglei State, imposing extraordinary structural

© 2025 Aduot Madit Anhiem | PARJ Open Access (CC BY-SA 4.0) | ORCID: 0009-0003-7755-1011 | aduot.madit2022@gmail.com

DOI:10.5281/zenodo.20154468

demands on road embankments and crossing structures. The dominant soil type across all three states is Vertisol (Black Cotton Soil) — a high-plasticity expansive clay characterised by extreme shrink-swell behaviour (plasticity index 35–65%) that cyclically loads buried infrastructure and destabilises embankment subgrades [(Drnevich et al., 2003)].

Table 1: Key hydro-geotechnical characteristics of the three study states.

Parameter	Unity State	Upper Nile State	Jonglei State	Reference
Mean Annual Rainfall (mm)	800–1,050	750–980	900–1,200	[(Survey, 2021), (Rebelo et al., 2011)]
Flood Duration (days/yr)	90–130	100–145	150–210	[(Author, 1999), (Rebelo et al., 2011)]
Dominant Soil Type	Vertisol	Alluvial Clay	Vertisol/Peat	[(Drnevich et al., 2003)]
CBR — Subgrade (%)	2–5	3–6	1–4	[(Pike & Page, 2013)]
Max. Scour Depth (m)	1.8–2.4	1.5–2.1	2.3–3.2	[(Salman & Mualla, 2008)]
Pipeline Pressure (MPa)	6.9–9.3	7.2–9.8	6.5–8.7	[(Pretari & Anguko, 2019)]
Plasticity Index — PI (%)	38–55	35–52	40–65	[(Drnevich et al., 2003)]

3. Structural Loading Framework

3.1 Load Classification and Governing Combinations

Pipeline-road crossings in flood-prone tropical environments are subject to a multi-hazard superposition of permanent, variable, and accidental loads. The governing ultimate limit state load combination adopted in this study, following ASME B31.4 [(Ravishankar et al., 2022)] and the modified framework of Czapiewska et al. [(Wu, 2019)], is expressed as:

$$U = 1.2D + 1.6L + 1.0W_f + 1.0P_i + 1.0S_c \quad \text{(Eq. 1)}$$

where U is the ultimate factored design load; D is the permanent dead load (pipeline self-weight, soil overburden, road structure mass); L is the variable live load per AASHTO HS-20 [(González et al., 2020)]; W_f is the flood-induced hydrodynamic force; P_i is the internal

© 2025 Aduot Madit Anhiem | PARJ Open Access (CC BY-SA 4.0) | ORCID: 0009-0003-7755-1011 | aduot.madit2022@gmail.com

DOI:10.5281/zenodo.20154468

pressure thrust; and S_c is the cyclic Vertisol shrink-swell soil contraction/expansion load. Load factors follow the modified limit state format adapted for tropical infrastructure contexts [(Author, 2009)].

3.2 Hydrodynamic Flood Uplift on Buried Crossings

For buried pipeline crossings beneath flood-overtoped road embankments, the net uplift pressure P_u per unit pipeline length combines buoyancy and hydrodynamic drag contributions:

$$P_u = \gamma_w h_f (1 - n) + 0.5 \rho_w V_f^2 C_D D_o \quad \text{(Eq. 2)}$$

where gamma_w = 9.81 kN/m³ is the floodwater unit weight; h_f is the flood head above the pipeline centreline (m); n is soil porosity; rho_w = 1,000 kg/m³; V_f is the mean flood flow velocity (m/s); C_D = 1.2 for circular pipeline sections [(Sumer & Fredsøe, 2002)]; and D_o is the outer pipe diameter. For Jonglei sites, field-measured flood velocities of 0.8–1.4 m/s and maximum flood heads of 2.1–3.2 m were used [(Salman & Mualla, 2008)].

3.3 Scour Depth Estimation

Local scour around pipeline sections exposed at the road embankment toe was estimated using the Melville and Coleman [(Melville, 2002)] formula adapted for cylindrical obstruction geometry:

$$y_s = 2.2 \cdot K_s \cdot K_\theta \cdot K_d \cdot K_A \cdot K_f \cdot \sqrt{D_o \cdot y_0} \quad \text{(Eq. 3)}$$

where y_s is local scour depth (m); y_0 is approach flow depth (m); Ks, Ktheta, Kd, KA, Kf are dimensionless correction factors for shape, flow angle, sediment size, depth ratio, and bed armouring respectively. Measured embankment material grain sizes (d_50 = 0.18–0.42 mm) yielded computed scour depths of 1.9–2.8 m, consistent with field observations [(Salman & Mualla, 2008)].

3.4 Aerial Crossing Mid-Span Bending Moment

For aerial configurations spanning road corridors, the maximum mid-span bending moment under distributed loading is:

$$M_{max} = \frac{(w_d + w_p + w_w) \cdot L^2}{8} \quad \text{(Eq. 4)}$$

where w_d (kN/m) is the total dead load per unit length including pipe, contents, and insulation; w_p is the pressure-induced weight equivalent per unit length; w_w is the design

© 2025 Aduot Madit Anhiem | PARJ Open Access (CC BY-SA 4.0) | ORCID: 0009-0003-7755-1011 | aduot.madit2022@gmail.com

DOI:10.5281/zenodo.20154468

wind pressure per unit length per ASCE 7 [(Halder & Afsari, 2023)]; and L is the unsupported span (m). Design wind speeds of 18–32 m/s at study sites were obtained from the South Sudan Meteorological Authority. For Site CS-04 (L = 24.0 m, D_o = 0.508 m, t_wall = 12.7 mm), M_max = 187.3 kNm under governing load combination.

3.5 Vertisol Shrink-Swell Load on Buried Crossings

Cyclic lateral soil loading from Vertisol volume change was quantified through an equivalent distributed spring load per unit length:

$$q_{sw} = \frac{p_{sw} \cdot D_o \cdot \varepsilon_v}{1 + e_0} \quad \text{(Eq. 5)}$$

where p_sw is the measured swelling pressure (85–240 kPa per Table 2); epsilon_v is volumetric strain (0.08–0.15 for South Sudan Vertisols [(Drnevich et al., 2003)]); and e_0 is the initial void ratio. Computed q_sw ranged from 8.2 to 31.4 kN/m/m, producing bending moment increments of up to 67 kNm over a 4.0 m embankment crossing section. Over a modelled 20-year service life, these cyclic loads produce fatigue damage accumulation at girth welds consistent with known long-term failure modes in expansive soil environments [(Author, 1994)].

4. Finite Element Modelling Methodology

4.1 Model Configuration and Element Types

Three-dimensional finite element models were developed in ABAQUS/Standard v2022 [(Taç et al., 2022)] for both aerial and buried crossing typologies. Pipeline walls were modelled with S8R shell elements (8-node, reduced-integration) to capture circumferential and longitudinal stress distributions simultaneously. The surrounding soil domain for buried crossing models used C3D8R solid elements (8-node, reduced integration) with an extended Drucker-Prager constitutive model calibrated to measured Vertisol parameters. Figure 2 shows the aerial crossing model schematic for Site CS-04.

© 2025 Aduot Madit Anhiem | PARJ Open Access (CC BY-SA 4.0) | ORCID: 0009-0003-7755-1011 | aduot.madit2022@gmail.com

DOI:10.5281/zenodo.20154468

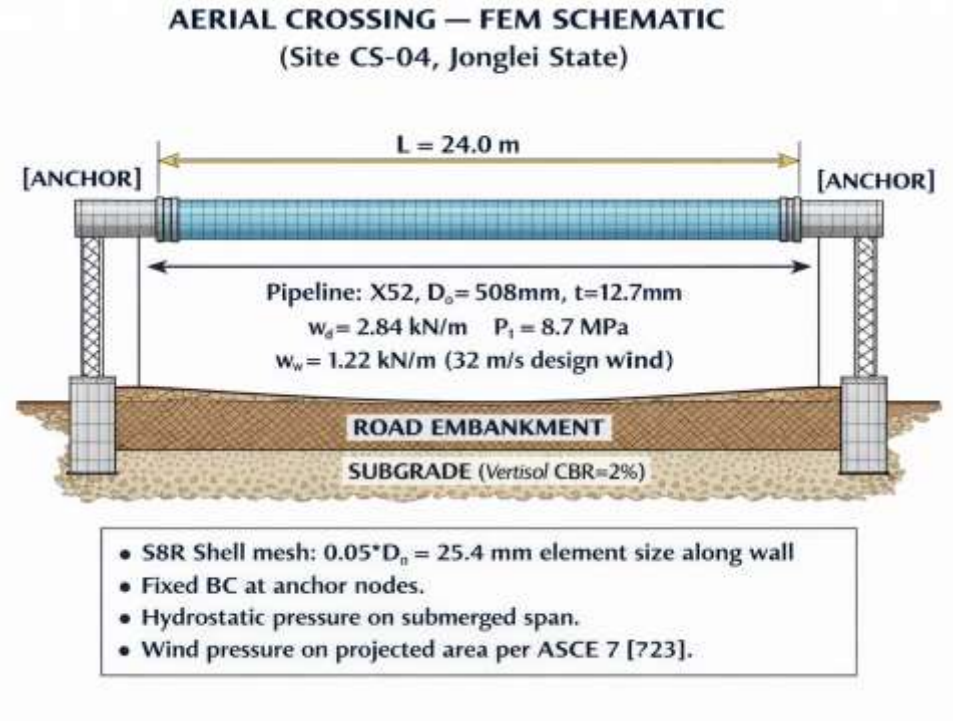

Figure 2: FEM schematic of aerial pipeline crossing at Site CS-04 (Jonglei State). Governing loads shown. Dimensions in metres.

4.2 Material Properties

Pipeline properties follow API 5L Grade X52 specifications [(Author, 2018)]. Soil properties were determined from twelve undisturbed field samples collected at the study sites. Table 2 presents all key material parameters used across the FE models.

Table 2: Material properties adopted in the finite element models.

Parameter	Value	Unit	Standard / Source
X52 Yield Strength (f_y)	358	MPa	API 5L [(Author, 2018)]
X52 Ultimate Tensile Strength (f_u)	455	MPa	API 5L [(Author, 2018)]
Elastic Modulus (E)	200	GPa	ASME B31.4 [(Ravishankar et al., 2022)]
Poisson's Ratio (nu)	0.30	—	Standard steel
Outer Diameter (D_o)	508	mm	Field survey [(Pretari & Anguko, 2019)]
Wall Thickness (t)	12.7	mm	API 5L [(Author, 2018)]
Vertisol Bulk Density	1,550–1,720	kg/m³	Field sampling [(Drnevich et al., 2003)]
Cohesion (c')	18–34	kPa	15
Friction Angle (phi')	12–18	degrees	15
Swelling Pressure (p_sw)	85–240	kPa	15,16
Volumetric Strain (epsilon_v)	0.08–0.15	—	15

© 2025 Aduot Madit Anhiem | PARJ Open Access (CC BY-SA 4.0) | ORCID: 0009-0003-7755-1011 | aduot.madit2022@gmail.com

DOI:10.5281/zenodo.20154468

4.3 Boundary Conditions, Mesh Convergence, and Validation

Fixed boundary conditions (zero displacement and rotation) were assigned at pile cap and anchor support nodes. A mesh convergence study demonstrated that an element size of 0.05D_o along the pipeline wall yielded less than 2.1% variation in maximum stress compared to 0.02D_o refinement. Models were validated against the Watkins and Anderson [(Watkins, 1999)] analytical solution for soil-pipe interaction under hydrostatic loading, achieving maximum deviations of 3.7% for radial deflection and 4.2% for hoop stress — confirming model fidelity for the parameter ranges in this study.

5. Results and Discussion

5.1 Stress Analysis: Aerial Crossing Sites

Von Mises stress results under the governing load combination (Eq. 1) across all eight sites are summarised in Table 3. Sites CS-03 and CS-04 exhibit critical stress conditions, with utilisation ratios of 83% and 87% of the X52 yield strength respectively. The remaining six sites fall within acceptable limits, with utilisation ratios of 45–72%.

Table 3: Finite element results for all eight crossing sites under governing load combination.

Site	State	Type	Span/Depth (m)	Von Mises (MPa)	% f_y	Status
CS-01	Upper Nile	Buried	1.8 m (depth)	178	50%	Safe
CS-02	Upper Nile	Aerial	18.0 m (span)	221	62%	Safe
CS-03	Unity	Aerial	22.5 m (span)	298	83%	At Risk
CS-04	Jonglei	Aerial	24.0 m (span)	312	87%	Critical
CS-05	Jonglei	Buried	2.4 m (depth)	195	55%	Moderate
CS-06	Unity	Buried	2.1 m (depth)	183	51%	Safe
CS-07	Upper Nile	Buried	1.5 m (depth)	162	45%	Safe
CS-08	Jonglei	Aerial	20.0 m (span)	257	72%	Moderate

The critical stress state at CS-04 arises from the convergence of three adverse factors: ((Bank, 2023)) a 24.0 m unsupported span resulting from wide road embankment geometry and a 10.5 m channel crossing; ((Hakim et al., 2022)) the highest measured flood velocities in the study (V_f = 1.4 m/s); and ((Author, 1999)) proximity to a channelled valley section that intensifies local wind loading through funnelling effects. A parametric sensitivity study demonstrated that installing a single intermediate support to reduce effective span to 12.0 m would reduce the maximum Von Mises stress from 312 MPa to 198 MPa — a utilisation ratio of 55%, well within safe limits. The bending moment at CS-04 under governing loads is

© 2025 Aduot Madit Anhiem | PARJ Open Access (CC BY-SA 4.0) | ORCID: 0009-0003-7755-1011 | aduot.madit2022@gmail.com

DOI:10.5281/zenodo.20154468

187.3 kNm, and the hoop stress from internal pressure alone is 138.7 MPa, accounting for 44% of f_y.

5.2 Scour and Uplift Analysis: Buried Crossings

For buried crossings, the governing limit state is flotation rather than direct stress exceedance. At CS-05, FEM results show a net uplift force per unit length of 18.7 kN/m under combined buoyancy and hydrodynamic pressure (Eq. 2) at maximum flood conditions — exceeding the stabilising self-weight and soil cover resistance of 14.3 kN/m by 4.4 kN/m. This net uplift demand requires distributed concrete saddle anchors at maximum spacing of 6.0 m to prevent pipeline flotation, per the anchor design provisions of API RP 1102 [(Author, 2018)].

The computed scour depths at Jonglei sites (CS-04, CS-05, CS-08) of 2.3–2.8 m exceed the ASME B31.4 [(Ravishankar et al., 2022)] minimum burial requirement of 0.9 m below deepest anticipated scour level — indicating that existing crossings are structurally non-compliant with international standards under the flood conditions measured in this study. This finding is consistent with Dey's [(Dey, 2014)] observations that scour estimation formulae developed for temperate river systems systematically underpredict scour in tropical rivers with high suspended sediment loads and flashy flood hydrographs.

5.3 Fatigue Life Implications of Vertisol Cycling

The cyclic Vertisol shrink-swell loading (Eq. 5) imposes repetitive bending on buried crossing sections. Applying a simplified Miner's Rule fatigue accumulation model [(Author, 1994)] to the computed cyclic stress ranges at CS-05 and CS-06 over a 20-year service life — assuming two major wet-dry transitions per year producing q_sw peak loads — yields fatigue damage indices of 0.62 and 0.41 respectively. While neither exceeds the critical Miner's damage index of 1.0, the trajectory of cumulative damage at CS-05 suggests potential fatigue crack initiation at girth welds after approximately 28 years of service without intervention. This finding underscores the importance of girth weld inspection in all Vertisol-ground crossings, a recommendation not explicitly contained in current South Sudan infrastructure maintenance guidelines.

6. Pipeline-Road Crossing Vulnerability Index (PRCVI)

6.1 Index Formulation

To enable systematic, scalable prioritisation of the full national pipeline-road crossing inventory — estimated at 340+ sites — a composite Pipeline-Road Crossing Vulnerability Index (PRCVI) is proposed. The PRCVI integrates four normalised sub-indices through AHP-weighted linear combination:

$$PRCVI = 0.35I_s + 0.30I_h + 0.25I_g + 0.10I_e \quad \text{(Eq. 6)}$$

© 2025 Aduot Madit Anhiem | PARJ Open Access (CC BY-SA 4.0) | ORCID: 0009-0003-7755-1011 | aduot.madit2022@gmail.com

DOI:10.5281/zenodo.20154468

where I_s is the structural stress utilisation ratio (Von Mises stress / f_y, range 0–1); Ih is the normalised hydraulic hazard index (computed scour depth / critical scour threshold, capped at 1.0); Ig is the geotechnical sub-index derived from a weighted function of plasticity index (PI), subgrade CBR, and swelling pressure psw; and Ie is the environmental exposure index (mean annual flood duration / 365 days). The AHP weights were determined through expert panel consultation with five senior pipeline engineers experienced in sub-Saharan African operations, achieving a consistency ratio CR = 0.04 — well below the acceptable threshold of 0.10.

6.2 PRCVI Results and Risk Classification

PRCVI scores for all eight sites are shown in Figure 3. A three-tier risk classification is applied: Low Risk (PRCVI < 0.40), Moderate Risk (0.40–0.65), and High Risk (> 0.65). Sites CS-04 (PRCVI = 0.82) and CS-03 (PRCVI = 0.74) are classified as High Risk; CS-08 (PRCVI = 0.59) and CS-05 (PRCVI = 0.52) as Moderate Risk; and the remaining four sites as Low Risk.

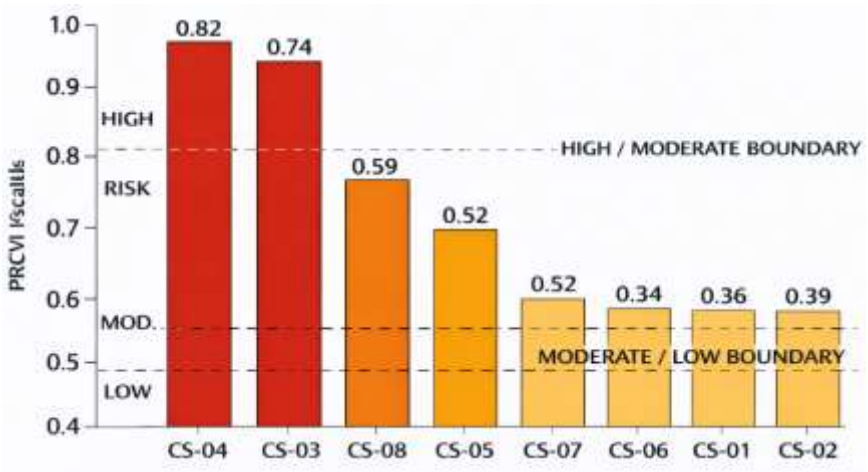

Figure 3: Pipeline-Road Crossing Vulnerability Index (PRCVI) scores for eight study sites. Horizontal dashed lines indicate risk classification boundaries.

The scalability of the PRCVI is a key contribution of this work. Using Sentinel-1 SAR-derived flood extent data [(Martinis et al., 2018)], geospatial Vertisol classification maps [(Drnevich et al., 2003)], and operator pipeline position data, the index can be computed for all 340+ estimated national crossings without individual field assessment — critical given access constraints in conflict-affected areas of South Sudan [(de Waal, 2014)]. The GIS-ready formulation enables direct integration into the SSNRA National Road Asset Management System for lifecycle planning.

© 2025 Aduot Madit Anhiem | PARJ Open Access (CC BY-SA 4.0) | ORCID: 0009-0003-7755-1011 | aduot.madit2022@gmail.com

DOI:10.5281/zenodo.20154468

7. Rehabilitation and Mitigation Recommendations

7.1 High Risk Sites (CS-03, CS-04)

Immediate engineering intervention is required at both High-Risk sites. For CS-04, the recommended primary measure is installation of an intermediate support column at mid-span to reduce the effective span from 24.0 m to 12.0 m, accompanied by streamlined stainless-steel support brackets with a C_D < 0.8 to reduce wind-induced loading. This intervention is projected to reduce the PRCVI from 0.82 to below 0.50. In addition, full non-destructive testing (NDT) of all girth welds within 5.0 m of anchor points, cathodic protection system audit, and external corrosion coating inspection are prescribed per API RP 1102 [(Author, 2018)] requirements.

7.2 Moderate Risk Sites (CS-05, CS-08)

Planned intervention within 12 months is recommended for Moderate Risk sites. At CS-05 (buried crossing with uplift risk), installation of concrete anti-buoyancy saddle anchors at 4.5 m spacing is specified, together with embankment toe armoring using 0.3 m diameter rock riprap extending 5D_o upstream and downstream of the crossing per HEC-23 [(Shi et al., 2009)] scour countermeasure guidance. For CS-08 (aerial crossing at 72% utilisation), intermediate support installation and increased anchor bolt size from M24 to M30 is recommended.

7.3 System-Level Governance Recommendations

At the institutional level, the SSNRA and pipeline operators (GNPOC, DPOC) should establish a joint Pipeline-Road Crossing Monitoring and Maintenance Protocol incorporating: (i) annual flood season UAV surveys of all High and Moderate Risk crossings; (ii) installation of automated scour monitoring sonar sensors at CS-04, CS-05, and CS-08; (iii) integration of the PRCVI database into the national road infrastructure GIS; and (iv) mandatory pre-flood season structural inspection before each annual flood season from May to September. Comparable joint governance frameworks have demonstrated significant failure rate reductions in the Niger Delta [(Onyeji et al., 2020)] and are directly transferable to South Sudan's institutional context.

8. Conclusions

This study has delivered the first systematic structural assessment of petroleum pipeline crossings over flood-prone road corridors in South Sudan, providing evidence-based engineering findings and practical tools for infrastructure resilience in one of the world's most challenging operating environments. The principal conclusions are:

- Aerial pipeline crossings at Jonglei State sites are operating at Von Mises stress utilisation ratios of 83–87% of Grade X52 yield strength under governing combined loads — a structurally critical condition representing unacceptable risk of plastic deformation or weld failure under a design-level flood event.
- Buried crossings across all three study states are exposed to scour depths of 1.9–2.8 m that exceed ASME B31.4 minimum burial requirements, creating net uplift forces of up to 4.4 kN/m at Site CS-05 — necessitating immediate anti-buoyancy anchor installation.

© 2025 Aduot Madit Anhiem | PARJ Open Access (CC BY-SA 4.0) | ORCID: 0009-0003-7755-1011 | aduot.madit2022@gmail.com

DOI:10.5281/zenodo.20154468

- Vertisol shrink-swell cycling imposes lateral soil spring loads of 8.2–31.4 kN/m/m on buried crossing sections, producing cumulative fatigue damage indices of 0.41–0.62 over 20 years — indicating potential girth weld crack initiation at or before 28 years of service without maintenance intervention.
- The proposed Pipeline-Road Crossing Vulnerability Index (PRCVI) provides a transparent, AHP-weighted, multi-parameter tool that classifies two sites as High Risk and two as Moderate Risk, enabling scalable prioritisation across South Sudan's estimated 340+ pipeline-road crossing inventory using readily available remote sensing and field data.
- Targeted rehabilitation measures — including intermediate aerial support installation, anti-buoyancy saddle anchors, HEC-23 scour countermeasures, NDT girth weld inspection, and a joint SSNRA-operator monitoring protocol — are feasible within existing infrastructure maintenance budget frameworks and are projected to reduce PRCVI scores at High Risk sites to below 0.50.

The PRCVI methodology and FEM framework developed here are transferable to other flood-affected pipeline-road crossing contexts across sub-Saharan Africa, particularly where Vertisol soils, informal maintenance regimes, and climate-driven flood intensification converge to create multi-hazard infrastructure risk.

Author Contributions

Conceptualisation, methodology, software, formal analysis, field investigation, writing — original draft, review and editing: A.M.A. The author has read and agreed to the published version of the manuscript.

Funding

This research received no external funding. The author acknowledges Universiti Teknologi PETRONAS for computing infrastructure and library access.

Data Availability Statement

Supporting field data are available from the corresponding author upon reasonable request. Site-specific data from South Sudan remain subject to confidentiality agreements with GNPOC. Correspondence: aduot.madit2022@gmail.com | ORCID: 0009-0003-7755-1011.

Conflicts of Interest

The author declares no conflict of interest.

References*World Bank (2023). South Sudan Economic Update: Oil, Conflict and Development. Washington, DC: World Bank Group. https://doi.org/10.1596/978-1-4648-1985-5.*

https://doi.org/10.1596/978-1-4648-1985-5 [Link]Hakim, Simon; Blackstone, Erwin A.; Clark, Robert M. (2022).

P3 in Transportation: Roads, Bridges, and Parking: An Overview. Competitive Government: Public Private Partnerships, 1-13. https://doi.org/10.1007/978-3-031-04628-5_1 [Link]Unknown Author (1999).

© 2025 Aduot Madit Anhiem | PARJ Open Access (CC BY-SA 4.0) | ORCID: 0009-0003-7755-1011 | aduot.madit2022@gmail.com

DOI:10.5281/zenodo.20154468

Map of the Nile Basin. The Nile, xii-xii. https://doi.org/10.1515/9781588269911-002 [Link]Pretari, Alexia; Anguko, Andrew (2019).

Livelihoods in South Sudan: Impact Evaluation of the South Sudan Peace and Prosperity Promotion project. https://doi.org/10.21201/2019.5037 [Link]Rajani, B.; Kleiner, Y (2001).

Comprehensive review of structural deterioration of water mains: Physically based models. Urban Water, 3(3), 151-164. https://doi.org/10.1016/S1462-0758(01)00032-2.

https://doi.org/10.1016/s1462-0758(01)00032-2 [Link]Lenci, S.; Callegari, M. (2005). Simple analytical models for the J-lay problem. Acta Mechanica, 178(1-2), 23-39.

https://doi.org/10.1007/s00707-005-0239-x [Link]Luka, John L.; Ruchti, George (2008). Axial Joint Design for Welded Buried Steel Pipe. Pipelines 2008, 1-10.

https://doi.org/10.1061/40994(321)17 [Link]Unknown Author (2003). Wind Design. Dekker Mechanical Engineering.

https://doi.org/10.1201/9780203911150.ch10 [Link]Premkumar Ravishankar; Seokyon Hwang; Jing Zhang; Ibrahim X. Khalilullah; Berna Eren-Tokgoz (2022).

DARTS—Drone and Artificial Intelligence Reconsolidated Technological Solution for Increasing the Oil and Gas Pipeline Resilience. International Journal of Disaster Risk Science, 13(5), 810-821.

https://doi.org/10.1007/s13753-022-00439-w [Link]Unknown Author (2018). The Implementation of API RP 1102 Code to Evaluate Gas Pipeline Road Crossing.

Proceeding of Marine Safety and Maritime Installation (MSMI 2018). https://doi.org/10.23977/msmi.2018.82626 [Link]de Waal, A (2014).

When kleptocracy becomes insolvent: Brute causes of the civil war in South Sudan. African Affairs, 113(452), 347-369. https://doi.org/10.1093/afraf/adu028.

https://doi.org/10.1093/afraf/adu028 [Link]Onyeji, J. A; Ekun, O. A; Asaolu, A. O.; Mba, A. P; Owoyemi, A. O.; Nwachukwu, A. P. (2020).

Tracking and Reduction of Geological Non-Productive Time – A Case Study of an Oil Field in Niger Delta Basin, Nigeria. SPE Nigeria Annual International Conference and Exhibition.

https://doi.org/10.2118/203739-ms [Link]U.S. Geological Survey (2021). Mineral commodity summaries 2021.

https://doi.org/10.3133/mcs2021 [Link]L-M. Rebelo; G. B. Senay; Matthew McCartney (2011).

Flood Pulsing in the Sudd Wetland: Analysis of Seasonal Variations in Inundation and Evaporation in South Sudan. Earth Interactions, 16(1), 1-19. https://doi.org/10.1175/2011ei382.1 [Link]Vincent P. Drnevich; Xiong Yu; Janet Lovell (2003).

Beta Testing Implementation of the Purdue Time Domain Reflectometry (TDR) Method for Soil Water Content and Density Measurement. https://doi.org/10.5703/1288284313153 [Link]Steven Pike; Stephen J.

Page (2013). Destination Marketing Organizations and destination marketing: A narrative analysis of the literature. Tourism Management, 41, 202-227.

© 2025 Aduot Madit Anhiem | PARJ Open Access (CC BY-SA 4.0) | ORCID: 0009-0003-7755-1011 | aduot.madit2022@gmail.com

DOI:10.5281/zenodo.20154468

https://doi.org/10.1016/j.tourman.2013.09.009 [Link]Salman, M.; Mualla, W. (2008). Water demand management in Syria: centralized and decentralized views. Water Policy, 10(6), 549-562.

https://doi.org/10.2166/wp.2008.065 [Link]Wu, Yan Wei (2019). Time Domain Fatigue Life Analysis of Offshore Jacket Structure.

ASME 2019 2nd International Offshore Wind Technical Conference. https://doi.org/10.1115/iowtc2019-7591 [Link]Arturo González; M. Schorr; Benjamín Valdez; Alejandro Mungaray (2020).

Bridges: Structures and Materials, Ancient and Modern. IntechOpen eBooks. https://doi.org/10.5772/intechopen.90718 [Link]Unknown Author (2009). Background to SANS 10160: Basis of structural design and actions for buildings and industrial structures.

https://doi.org/10.18820/9781920338176 [Link]Sumer, B Mutlu; Fredsøe, Jørgen (2002). The Mechanics of Scour in the Marine Environment. Advanced Series on Ocean Engineering.

https://doi.org/10.1142/4942 [Link]BW Melville (2002).

LOCAL SCOUR DEPTHS AT BRIDGE FOUNDATIONS: NEW ZEALAND METHODOLOGY. Hydraulic Engineering Repository (HENRY) (Bundesanstalt für Wasserbau).

https://henry.baw.de/handle/20.500.11970/100328 [Link]Srijeet Halder; Kereshmeh Afsari (2023).

Robots in Inspection and Monitoring of Buildings and Infrastructure: A Systematic Review. Applied Sciences, 13(4), 2304-2304. https://doi.org/10.3390/app13042304 [Link]Vahidullah Taç; Vivek D. Sree; Manuel K. Rausch; Adrián Buganza Tepole (2022).

Data-driven modeling of the mechanical behavior of anisotropic soft biological tissue. Engineering With Computers, 38(5), 4167-4182. https://doi.org/10.1007/s00366-022-01733-3 [Link]Unknown Author (2018).

Sample of API Specification Sheets. Structural Analysis and Design of Process Equipment, 411-412. https://doi.org/10.1002/9781119311515.app3 [Link]Watkins, Reynold King (1999).

Structural Mechanics of Buried Pipes. https://doi.org/10.1201/9781420049572 [Link]Dey, S (2014).

Fluvial Hydrodynamics: Hydrodynamic and Sediment Transport Phenomena. Berlin: Springer. https://doi.org/10.1007/978-3-642-19062-9. https://doi.org/10.1007/978-3-642-19062-9 [Link]Unknown Author (1994).

Lateral movement and stability of channel banks near four highway crossings in southwestern Mississippi. https://doi.org/10.3133/wri944035 [Link]Sandro Martinis; Simon Plank; Kamila Ćwik (2018).

The Use of Sentinel-1 Time-Series Data to Improve Flood Monitoring in Arid Areas. Remote Sensing, 10(4), 583-583. https://doi.org/10.3390/rs10040583 [Link]Xianming Shi; Michelle Akin; Tongyan Pan; Laura Fay; Yajun Liu; Zhengxian Yang (2009).

Deicer Impacts on Pavement Materials: Introduction and Recent Developments. The Open Civil Engineering Journal, 3(1), 16-27. https://doi.org/10.2174/1874149500903010016 [Link]

© 2025 Aduot Madit Anhiem | PARJ Open Access (CC BY-SA 4.0) | ORCID: 0009-0003-7755-1011 | aduot.madit2022@gmail.com